Nonproportionality of Scintillator Detectors: Theory and Experiment

Stephen A. Payne, Nerine J. Cherepy, Giulia Hull, John D. Valentine, *Senior Member, IEEE,* William W. Moses, *Fellow IEEE* and Woon-Seng Choong, *Member, IEEE*

***Abstract*—On the basis of nonproportionality data obtained for several scintillators, we have developed a theory to describe the carrier dynamics to fit the light yield versus electron energy. The theory of Onsager was adapted to explain how the carriers form excitons or sequentially arrive at the activators to promote the ion to an excited state, and the theory of Birks was employed to allow for exciton-exciton annihilation. We then developed a second theory to deduce the degradation in resolution that results from nonproportionality by evoking Landau fluctuations, which are essentially variations in the deposited energy density that occur as the high energy electron travels along its trajectory. In general there is good agreement with the data, in terms of fitting the nonproportionality curves and reproducing the literature values of nonproportionality's contribution to the scintillator resolution.**

***Index Terms*—Nonproportionality, Scintillators, Radiation Detector**

I. Introduction

With the resurgence of interest in developing scintillator detectors that have good energy resolution, an improved understanding of nonproportionality has become a crucial matter since it presents the fundamental limit to the achievable resolution [1]-[4]. In order to hasten an improved understanding of scintillator nonproportionality, we have constructed an instrument referred to as SLYNCI (Scintillator Light Yield Nonproportionality Compton Instrument). This is a second-generation instrument to the original device developed by Valentine and coworkers [5], wherein several new principles of operation have served to increase the data rate by an order of magnitude as discussed in detail in Refs. [6]-[8]. In the present article, the focus is on a theory to describe the measured electron response, which is the light yield as a function of the electron energy. To do this, we account for transport of carriers and excitons, in terms of how they transfer their energy to the activators with competition from nonradiative decay pathways. This work builds on the original work of Murray and coworkers [9], and on the understanding of excitons [10]. We then provide a new theoretical framework from which the nonproportionality data is reduced to a measure of the degradation in resolution.

This work was supported in part by the Department of Homeland Security, Domestic Nuclear Detection Office and in part by the National Nuclear Security Administration, Office of Defense Nuclear Nonproliferation, Office of Nonproliferation Research and Development (NA-22) of the U.S. Department of Energy. This work was performed by Lawrence Livermore National Laboratory under contract DE-AC52-07NA27344 and by Lawrence Berkeley National Laboratory under Contract No. DE-AC02-05CH11231.

S. Payne is with Lawrence Livermore National Laboratory (LLNL), Livermore, CA 94551 USA (e-mail: payne3@llnl.gov).

N. Cherepy is also with LLNL (e-mail: cherepy1@llnl.gov).

G. Hull was previously with LLNL and can currently be reached at giulia.hull@gmail.com.

J. Valentine was previously with LLNL and is currently at SAIC, San Diego. He can be reached at john.d.valentine@saic.com.

W. Moses is at Lawrence Berkeley National Laboratory (LBNL), Berkeley, CA 94720 USA (e-mail: wwmoses@lbl.gov).

S. Choong is at Lawrence Berkeley National Laboratory (LBNL), Berkeley, CA 94720 USA (e-mail: wschoong@lbl.gov).

II. Background

The basic equation describing the number of photoelectrons produced in the photodetector of a scintillator is [11]:

$$n_{PE} = \left(\frac{E_\gamma}{\beta \; E_{GAP}} \right) \eta_{CAP} \eta_{PH} \tag{1}$$

where E_γ / β E_{GAP} is the number of electron-hole pairs generated with E_γ being the gamma energy and E_{GAP} the scintillator bandgap, β is a constant, η_{CAP} is the efficiency by which the carriers' energy is captured by the activators, and η_{PH} is the efficiency by which the activators emit photons which are subsequently collected and photodetected. Accordingly the relative variance in the number of photoelectron pulses of the scintillator instrument is given by:

$$\left(\frac{\delta n_{PE}}{n_{PE}} \right)^2 = \left[\frac{\delta \left(\frac{E_\gamma}{\beta \; E_{GAP}} \right)}{\left(\frac{E_\gamma}{\beta \; E_{GAP}} \right)} \right]^2 + \left[\frac{\delta \eta_{CAP}}{\eta_{CAP}} \right]^2 + \left[\frac{\delta \eta_{PH}}{\eta_{PH}} \right]^2 + \left[\frac{\delta n_{NOISE}}{n_{PE}} \right]^2 \tag{2}$$

where the electronic noise term is conventionally added in an *ad hoc* manner, and the resolution is simply the square root of this expression. This paper will be mainly concerned with the ($\delta\eta_{CAP}$ / η_{CAP}) term since it determines the nonproportionality, but for completeness we offer the values of the other terms on the right-hand-side (RHS) of the

equation. From semiconductor physics we know that:

$$\left[\frac{\delta\left(\frac{E_\gamma}{\beta\ E_{GAP}}\right)}{\left(\frac{E_\gamma}{\beta\ E_{GAP}}\right)}\right] = \left[\frac{F}{\left(\frac{E_\gamma}{\beta\ E_{GAP}}\right)}\right]^{1/2} \quad (3)$$

where F is the Fano factor (~0.1) and β ~ 3.0. The impact of this term on scintillator resolution is negligible. The photon statistics term is:

$$\left[\frac{\delta\ \eta_{PH}}{\eta_{PH}}\right] = \left[\frac{1-\eta_{PH}}{\eta_{PH}\eta_{CAP}\left(\frac{E_\gamma}{\beta\ E_{GAP}}\right)}\right]^{1/2} \quad (4)$$

where the denominator is just n_{PE}. The numerator contains the 1 - η_{PE} value in order to convert the usual Poisson statistics [12] to the binomial formulation, as is required for the photoelectron efficiency η_{PH} being large, greater than about 0.5. The binomial statistical treatment models the limit as η_{PH} → 1 correctly, in that the variance goes to zero (since trivially there can be no variance if every excited state is registered as a collected / detected photon). A caveat in the use of Eq. (4) concerns the operation of avalanche photodiodes [13-15], where researchers often introduce an "added noise factor" into the numerator (F_{APD}), where its value typically is in the range of 1.5 – 2. For photomultiplier tubes (PMT), a related factor, usually expressed at 1 + ε (with ε ~ 0.1), is sometimes included to account for the electron-multiplication instabilities of the PMT. It is noteworthy that, in principle, scintillators can have resolution rivaling semiconductors if nearly 100% photon detection were achieved with a noiseless detector, were it not for the impact of nonproportionality.

III. Theory of Nonproportionality in the Light Yield

Fig. 1 depicts the collisional cascade with the myriad of physical processes that transpire (Compton scatter, photoelectric interaction, delta rays, x-ray fluorescence, Auger electrons, etc.), formation of excitons that are believed to become self-trapped in most insulators (i.e. self-trapped excitons, STE), transfer of energy to activators by way of carrier or exciton migration, and photon emission. Given the supply of electron-hole pairs, nonproportionality of scintillators is modeled by considering the competing influences on the energy capture efficiency at activators:

- Recombination of electron and holes at activators and to form excitons
- Exciton-exciton annihilation and other exciton and carrier losses

Whether the electrons and holes recombine to form excitons that migrate to activators and transfer their energy, or sequentially arrive at activators to confer their energy, the process of electron-hole recombination has traditionally been described by the so-called Onsager mechanism [16] for many physical systems. The electron and hole may or may not recombine depending on the Onsager radius (r_{ONS}), or the point where the Coulombic and thermal energies match:

$$\frac{e^2}{\varepsilon\ r_{ONS}} = kT \quad (5)$$

where ε is the dielectric constant, *e* is the elemental electron charge, and kT is the thermal energy. The electron-hole pairs may be separated by a distance less than or larger than r_{ONS} initially. The probability of recombination is most simply described with [16]:

$$P_{RECOMB} = 1 - \exp\left(\frac{-r_{ONS}}{r_{e/h}}\right) \quad (6)$$

where $r_{e/h}$ is the initial electron-hole separation. In this model, electrons and holes that do not succumb to the Coloumbic force are lost. We can take $r_{e/h}$ to be the average electron-hole separation, $\beta E_{GAP}/(dE/dx)$, for each short segment of the electron trajectory. Therefore:

$$\eta_{ONS} = 1 - \eta_{EXC}\exp\left(\frac{-\frac{dE}{dx}}{\left(\frac{dE}{dx}\right)_{ONS}}\right) \quad (7)$$

where $(dE/dx)_{ONS} = \beta\ E_{GAP} / r_{ONS}$. Eq. (7) allows distinction for the fraction (1 - η_{EXC}) of excitons that are "born" during the cascade and up to η_{EXC} to be "created" by electron-hole recombination. It should be emphasized that the Onsager mechanism equivalently accounts for recombination of carriers sequentially at the activators, which also generates excited states. Fig. 2 contains a simple illustration of electron-hole generation with exciton formation and exciton-exciton annihilation along the track; the Onsager mechanism of recombination is portrayed on the RHS. Our model in essence reduces the physical problem to a single dimension (x), constrained along the electron trajectory.

The competing process of exciton-exciton annihilation (Fig. 2) has historically been described by the Birks equation [17]:

$$\eta_{BIRKS} = \left[1 + \left(\frac{\left(\frac{dE}{dx}\right)}{\left(\frac{dE}{dx}\right)_{BIRKS}}\right)\right]^{-1} \quad (8)$$

where dE/dx is a measure of the exciton concentration (i.e. based on their separation along the high-energy electron trajectory) and $(dE/dx)_{BIRKS}$ is an empirical fitting parameter relating to the strength of the exciton-exciton annihilation mechanism (usually considered to arise from Auger

processes).

Eqs. (7) and (8) are finally multiplied ($\eta_{CAP} = \eta_{ONS}\ \eta_{BIRKS}$) to yield the equation used to describe the light yield at a particular electron energy, E, (corresponding to a particular dE/dx):

$$\eta_{CAP}\left(\frac{dE}{dx}\right) = \eta_{CAP}^{0}\,\frac{1-\eta_{EXC}\exp\left[-\left(\frac{dE}{dx}\right)\Big/\left(\frac{dE}{dx}\right)_{ONS}\right]}{1+\left[\left(\frac{dE}{dx}\right)\Big/\left(\frac{dE}{dx}\right)_{BIRKS}\right]} \qquad (9)$$

The η_{CAP} factor accounts for the first-order nonradiative losses for carriers and excitons. However, now we must remember that the high-energy electron created by the gamma photon must be integrated along its trajectory from the initial energy, E_0, to the final ionization energy I (defined by the classic Bethe-Bloch equation, see below):

$$\left[\eta_{CAP}(E_0)\right]_T = \int_{E_0}^{I}\left[\eta_{CAP}\,dE \Big/ (E_0 - I)\right] \qquad (10)$$

The last ingredient needed to fit the actual experimental data is the Bethe-Bloch equation [18] which relates dE/dx to E:

$$\frac{dE}{dx} = \frac{2\pi\, e^4 \rho_e}{E}\,\ell n\left(\frac{1.16\,(E+cI)}{I}\right) \qquad (11)$$

where ρ_e is the electron density given by $\rho Z/MW$ (ρ = mass density, Z is the additive atomic number of all elements in the compound, and MW is the molecular weight), and the extra cI term has been added for greatly improved accuracy at low energies (analyzed further below). In order to empirically assess the value of *c*, we fit our nonproportionality data on $LaBr_3$(Ce) for various values of *c*, as shown in Fig. 3. (In actuality, we have employed the relativistic form of the Bethe-Bloch equation [12], substituting E → E + cI into this equation.) It is seen that the best fits are obtained for values of 2.8 and 4.2; the c = 0 case breaks down as expected, since the Bethe-Bloch form presupposes $E_0 >> I$. To further define the suitable *c* value, we can compare the Bethe-Bloch equation with the detailed calculations of Vasil'ev [19], where the polarization approximation is used for to calculate dE/dx for NaI. Since c = 4.2 appears too large in Fig. 4 and noting that the theory of Ref. [19] employs several approximations, we settle on using c = 2.8. Although some ambiguity in choosing this magnitude remains, the selected value is reasonable for the purposes of this development.

Having now established all of the ingredients needed for fitting the experimental data, Fig. 5 displays the comparison of the data with our model. It is seen that good fits are achievable in all cases for the SLYNCI data: $LaBr_3$(Ce), $LaCl_3$(Ce), NaI(Tl), SrI_2(Eu), $YAlO_3$(Ce) or YAP(Ce), and $Y_3Al_5O_{12}$(Ce) or YAG(Ce). Several of the scintillators have previously been studied by Valentine and coworkers [20]-[23]. The parameters are summarized in Table I, where we also include the fits to several nonproportionality data from the literature, including $Bi_4Ge_3O_{12}$ (BGO) and Lu_2SiO_5(Ce) or LSO [24]. Two sources of NaI(Tl) samples are considered, which evidence reproducibly different responses [25]. The ionization energies, I, were obtained from the NIST website [26].

By examining the data in Table I, we can see that the $(dE/dx)_{ONS}$ values are similar, while the larger η_{ONS} values correspond to scintillators that evidence a more pronounced "rise" in light yield to lower electron energy (i.e. right to left), and the smaller $(dE/dx)_{BIRKS}$ values indicate compounds with a more abrupt "fall" toward the lowest electron energies. All scintillators apparently experience some amount of electron-hole recombination as evidenced by the non-zero values of η_{ONS}; the prominence of the "rise" is dictated by the competition between exciton formation and exciton-exciton annihilation. Finally, as noted in a prior publication [25], there can be measurable variation in the nonproportionality data among samples of the same basic composition, as is found to be the case for NaI(Tl), particularly for the magnitude of the $(dE/dx)_{BIRKS}$ parameter which is likely sensitive to the presence of unintended impurities, defects, and the activator concentration.

TABLE I

FITTING PARAMETERS EMPLOYED TO FIT THE DATA IN FIG. 5, AS WELL AS FOR SEVERAL NONPROPORTIONALITY DATA SETS REPORTED IN THE LITERATURE [24]. THE DENSITY AND IONIZATION ENERGY ARE ALSO REPORTED.

Scintillator	$(dE/dx)_{ONS}$ (cm/MeV)	η_{ONS} (%)	$(dE/dx)_{BIRKS}$ (cm/MeV)	ρ (g/cm^3)	I (keV)
$LaBr_3$(Ce)	34.5	19	439	5.06	0.455
$LaCl_3$(Ce)	26.3	16	465	3.79	0.329
NaI(Tl) #1	26.0	45	263	3.6	0.466
NaI(Tl) #2	27.8	44	339	3.6	0.466
SrI_2(Eu)	27.8	22	526	4.6	0.513
YAP(Ce)	27.0	8	741	5.55	0.239
YAG(Ce)	27.0	8	541	4.6	0.218
LSO(Ce)	26.3	14	208	7.4	0.472
BGO	27.0	10	455	7.1	0.534

We can independently estimate the magnitude of $(dE/dx)_{ONS}$ by employing:

$$\left(\frac{dE}{dx}\right)_{ONS} = \frac{(\beta\, E_{GAP})(\varepsilon\, kT)}{e^2} \qquad (12)$$

where ε = 7.3, E_{GAP} = 6.6 eV, and β = 3.8 for NaI, leading to the estimate that $(dE/dx)_{ONS}$ = 33 MeV/cm compared to the fitted values of 26.0 - 27.8 MeV/cm, offering substantial

support for of the proposed mechanism.

IV. Theory of Resolution Degradation due to Nonproportionality

We are now ready to explore nonproportionality's contribution to the resolution of a scintillator. It is recognized to consist of two independent phenomena relating to: (1) variations in the distribution of primary electrons created by the gamma photon ($\delta\eta_\gamma$), and (2) fluctuations in the dE/dx of the high-energy electrons along their trajectory [5,20,23]:

$$\delta\,\eta_{NonP}^{2} = \delta\,\eta_{\gamma}^{2} + \delta\,\eta_{CAP}^{2} \tag{13}$$

The $\delta\eta_\gamma$ term arises from variations in the excitation processes possible, leading to the generation of several electrons with different energies that access various energies in the nonproportionality light yield curves. This has been studied in detail by Valentine and coworkers for NaI(Tl) and appears to be a significant but only partial contributor to the resolution [23]. In this paper we focus our attention on the fluctuations in the electron trajectory [27], assuming that it is initiated with a single high-energy electron having the full gamma energy (E_0). It is necessary to sum these fluctuations in quadrature along the electron trajectory (since they are expected to be uncorrelated) to obtain the resolution:

$$R_{NonP} = \left(\frac{\delta\eta_{CAP}}{\eta_{CAP}}\right)_T = \left[\frac{\int_{E_0}^{I}\left(\frac{\delta\eta_{CAP}(E)}{\eta_{CAP}(E)}\right)^2 dE}{(E_0 - I)}\right]^{1/2} \tag{14}$$

In order to evaluate this integral, we must first reformulate the parenthetical quantity in the numerator of the integrand as:

$$\frac{\delta\,\eta_{CAP}}{\eta_{CAP}} = \frac{1}{\eta_{CAP}}\left(\frac{d\,\eta_{CAP}}{d\left(dE/dx\right)}\right)\delta\left(\frac{dE}{dx}\right) \tag{15}$$

where the magnitude of $d\eta_{CAP}/d(dE/dx)$ can be numerically evaluated from the fitted nonproportionality curves, together with the Bethe-Bloch equation. Now we need to deduce a value for the fluctuations in the ionization rate, which fortunately has been previously analyzed by Landau, given by (in terms of the full-width-at-half-maximum, FWHM):

$$\delta\left(\frac{dE}{dx}\right)_{FWHM} = 3.6\left(\frac{2\pi\,e^4\rho_e}{E}\right) \tag{16}$$

The Landau distribution for stopping power fluctuations can be evaluated with [28]:

$$L = (2\pi)^{-1/2}\left(\frac{2\pi\,e^4\rho_e}{E}\right)^{-1}\exp\{-(1/2)[\Delta + \exp(-\Delta)]\} \tag{17}$$

where

$$\Delta = \left(\frac{2\pi\,e^4\rho_e}{E}\right)^{-1}\left[\left(\frac{dE}{dx}\right) - \left(\frac{dE}{dx}\right)_{BETHE}\right] \tag{18}$$

and $(dE/dx)_{BETHE}$ is the usual peak value of the stopping power from the conventional Bethe-Bloch equation. Once again we face the difficulty that this function becomes inaccurate at low energies, a situation which we attempt to remedy by using the same substitution utilized above (vide infra): E → E + cI. From Fig. 6, where the distributions are plotted for several electron energies, we see that the low energy correction begins to have an impact at 3 keV. The factor of 3.6 appearing in Eq. (16) was determined by examining the shapes of these curves, to convert the parenthetical term in Eq. (16) to a FWHM.

We now have the tools needed to calculate the contribution of electron nonproportionality to the gamma resolution on the basis of Eqs. (14-16) with the parameters derived from the fits to the nonproportionality data (using c=2.8 in the Bethe-Bloch and Landau equations). These results are listed in Table II and compared with data from the literature.

From the data in Table II, we can see that, first of all, the R_{NonP} values have the correct general magnitudes, and also that they faithfully reproduce the rank ordering of scintillator materials. Interestingly, $LaCl_3$(Ce) has superior nonproportionality to $LaBr_3$(Ce) but also lower light yield. SrI_2(Eu) has excellent proportionality, while also offering extremely high light yield (~100,000 photons/MeV). LSO, on the other hand, is quite nonproportional but is mainly deployed in PET scanners where time-resolution and stopping power are the key parameters rather than resolution. We find that the goal of attaining excellent resolution is optimized by balancing the Onsager and Birks mechanisms to yield a somewhat flatter electron response.

We find the agreement in Table II to be encouraging. However, it is noteworthy that the purpose of the fits of Fig. 5 turns out to be the extrapolation to the crucial low energy regime, introducing some uncertainty in the calculated resolution. The reader should be cautioned that the literature values also carry significant error, noting that they are deduced by essentially accounting for all contributions to

TABLE II
Calculated and Measured Values of the Nonproportionality at 662 keV, Based on Refs. [14], [15], [29]-[33]

Scintillator	R_{NonP} (%) Calculated	R_{NonP} (%) Literature
$LaBr_3$(Ce)	2.52	1.6
$LaCl_3$(Ce)	2.27	1.4
NaI(Tl) #1	4.64	5.9
NaI(Tl) #2	4.44	
SrI_2(Eu)	2.30	<2.0
YAP(Ce)	2.43	2.5 +/-1
YAG(Ce)	2.85	Unknown
LSO(Ce)	5.93	6.6
BGO	3.21	4.1

resolution and then attributing the remainder to nonproportionality; moreover some sample-to-sample variation may be expected. At this juncture, we can say that we are satisfied with the results of our first attempt to produce a comprehensive theory of scintillator nonproportionality, although we recognize that there may well be further improvements and insights in the future.

V. Summary

We have utilized data obtained from SLYNCI to obtain accurate nonproportionality data on several scintillators, and have developed a theory to describe the carrier dynamics to fit the data for the light yield versus electron energy. To accomplish this, the theory of Onsager was adapted to explain how the carriers form excitons or sequentially arrive at the activators to promote the ion to an excited state. Furthermore, the theory of Birks was employed to allow for exciton-exciton annihilation, particularly at the lowest electron energies. Importantly, we found that both of these mechanisms are operative in all scintillator materials, while their relative magnitudes can vary. We then develop a second theory to deduce the degradation in resolution that results from nonproportionality by evoking the influence of Landau fluctuations, which are essentially variations in the deposited energy density that occur as the high energy electron travels along its trajectory. There is good agreement with the data in general, in terms of fitting the nonproportionality curves and reproducing the literature values of nonproportionality's contribution to the scintillator resolution.

Acknowledgment

We would like to thank Andrey Vasil'ev (Moscow State University) for sharing his original computation of the dE/dx for NaI, Richard Williams for discussions on the Onsager mechanism and the behavior of excitons, and Kanai Shah of RMD for providing the SrI_2(Eu) crystal.

References

[1] J. E. Jaffe, D. V. Jordan and A. J. Peurrung, "Energy nonlinearity in radiation detection materials: Causes and consequences," *Nuclear Instruments and Methods in Physics Research A,* vol. 570, pp. 72-83, 2007.
[2] S. E. Derenzo, M. J. Weber, E. Bourret-Courchesne, and M. K. Klintenberg, "The quest for the ideal inorganic scintillator," *Nuclear Instruments and Methods in Physics Research A*, vol 505, pp. 111-117, 2003.
[3] C. L. Melcher, "Perspectives on the future of development of new scintillators," *Nuclear Instruments and Methods in Physics Research A*, vol. 537, pp. 6-14, 2005.
[4] J. E. Jaffe, "Energy and length scales in scintillator nonproportionality," *Nucl. Instr. & Meth. A, vol.* 580, 1378-1382 (2007).
[5] J. D. Valentine, B. D. Rooney and J Li, "The light yield nonproportionality component of scintillator energy resolution," *IEEE Transactions on Nuclear Science,* vol. 45, pp. 512-517, 1998.
[6] W.-S. Choong, K.M. Vetter, W.W. Moses, S.A. Payne, N.J. Cherepy, J.D. Valentine and G. Hull, "Design of a Facility for Measuring Scintillator Non-Proportionality," *IEEE Trans. Nucl. Sci*., vol. 55, pp. 1753-1758, 2008.
[7] W.-S. Choong, G. Hull, W.W. Moses, K.M. Vetter S.A. Payne, N.J. Cherepy, J.D. Valentine, "Performance of a Facility for Measuring Scintillator Non-Proportionality," *IEEE Trans. Nucl. Sci*., vol. 55, pp. 1073-1078, 2008.
[8] G. Hull, S. Du, T. Niedermayr, S. Payne, N. Cherepy, A. Drobshoff, and L. Fabris "Light Collection Optimization in Scintillator Based Gamma-Ray Spectrometers" *Nucl. Instr. Meth. A*, vol. 588, 384-388, 2008.
[9] R. B. Murray and A. Meyer, "Scintillation response of activated inorganic crystals to various charged particles," Phys. Rev. **112**, 815-826, 1961; H. B. Dietrich and R. B. Murray, "Kinetics of the diffusion of self-trapped holes in alkali halide scintillators," *Journal of Luminescence,* vol. 5, pp. 155-170, 1972.
[10] K. S. Song and R. T. Williams, *Self-Trapped Excitons*, Springer, 1996.
[11] A. Lempicki, A J. Wojtowocz, and E. Berman, "Fundamental limits of scintillator performance," *Nucl. Instr. Meth*. A**,** vol. 333, pp. 304-311, 1993.
[12] G. F. Knoll, *Radiation Detection and Measurements*, John Wiley and Sons, Inc., New York, 1999.
[13] M. Moszynski, M. Szawlowski, M. Kapusta and M. Balcerzyk, "Avalanche photodiodes in scintillation detection," *Nuclear Instruments and Methods in Physics Research A*, vol. 497, pp. 226-233, 2003.
[14] M. Moszynski, M. Kapusta, D. Wolski, M. Szawlowski and W. Klamra, "Energy resolution of scintillation detectors readout with large area avalanche photodiodes and photomultipliers," *IEEE Transactions on Nuclear Science,* vol. 45, pp. 472-477, 1998.
[15] M. Moszynski, M. Kapusta, M. Balcerzyk, M. Szawlowski, D. Wolski, I. Wegrzecka and M. Wegrzecka, "Comparative study of avalanche photodiodes with different structures in scintillation detection," *IEEE Transactions on Nuclear Science*, vol. 48, pp. 1205-1210, 2000.
[16] For example, see Eq. 27 of G. J. Hoffman and A. C. Albrecht, "Near threshold photoionization spectra in nonpolar liquids: A geminate pair based model," *J. Phys. Chem*., vol. 95, pp. 2231-2241, 1991; and A. A. Neufeld, A. I. Burshtein, G. Angulo and G. Grampp, "Viscosity dependence of geminate recombination efficiency after bimolecular charge separation," *Journal of Chemical Physics*, vol. 116, pp. 2472-2479, 2002.
[17] J. B Birks, *Theory and Practice of Scintillation Counting,* Pergamon Press, Oxford, 1964.
[18] A. Jablonski, S. Tanuma, and C. J. Powell, "New universal expression for the electron stopping power for energies between 200 eV and 30 keV," *Surface and Interface Analysis,* vol. 38, pp. 76-83, 2006.
[19] A. N. Vasil'ev, "From luminescence non-linearity to scintillation non-proportionality," *IEEE Transaction in Nuclear Science***,** vol. 55, pp. 1054-1061, 2008; A. N. Vasilev, IEEE Trans. Nucl. Science (2008) in press; G. Bizarri, W. W. Moses, J. Singh, A. N. Vasil'ev, and R. T. Williams, "The role of different linear and nonlinear channels of relaxation in the scintillator non-proportionality," *Journal of Luminescence*, to be published.
[20] W. Mengesha and J. D. Valentine, "Benchmarking NaI(Tl) electron energy resolution measurements," *IEEE Transactions on Nuclear Science,* vol. 49, pp. 2420-2426, 2002.
[21] W. Mengesha, T. D. Taulbee, B. D. Rooney, and J. D. Valentine, "Light Yield Nonproportionality of CsI(Tl), CsI(Na), and YAP," *IEEE Transaction on Nuclear Science* vol. 45, pp. 456-461, 1998.
[22] E. V. D. van Loef, W. Mengesha, J. D. Valentine, P. Dorenbos, and C. W. E. Van Eijk, "Non-proportionality and energy resolution of a $LaCl_3$:10% Ce^{3+} scintillation crystal," *IEEE Transactions on Nuclear Science*, vol. 50, pp. 155-158, 2003.
[23] M. Moszynski, J. Zalipska, M. Balcerzyk, M. Kapusta, W. Mengesha, and J. D. Valentine, "Intrinsic energy resolution of NaI(Tl)," *Nuclear Instruments and Methods in Physics research A***,** vol. 484, pp. 259-269, 2002.
[24] T. D. Taulbee, B. D. Rooney, W. Mengesha and J. D. Valentine, "The measured electron response nonproportionalities of CaF_2, BGO, and LSO," *IEEE Transactions on Nuclear Science*, vol. 44, pp. 489-493, 1997.
[25] G. Hull, W.-S. Choong, W. W. Moses, G. Bizarri, J. D. Valentine, S. A. Payne, N. J. Cherepy, and B. W. Reutter, "Measurements of NaI(Tl) electron response: comparison of different samples," *IEEE Transactions in Nuclear Science*, in press.
[26] Available on NIST website - http://physics.nist.gov/PhysRefData/Star/Text/ESTAR-u.html
[27] M. Marsman, P. Dorenbos, and C. W. E. van Eijk, "A theoretical approach to the non-proportional gamma energy response of scintillators," *Proceedings of the International Conference on Inorganic Scintillators and Their Applications*, Delft, The Netherlands, August 28 – September 1, 1995, p 156-158.
[28] J. E. Moyal, "Theory of ionization fluctuations," *Philosophical Magazine* vol 46, pp. 263-280, 1955.
[29] C. W. E. van Eijk, P. Dorenbos, E. V. D. Van Loef, K. Kraemer, and H. U. Guedel, "Energy resolution of some new inorganic-scintillator gamma-ray detectors," *Radiation Measurements,* vol. 33, pp. 521-525, 2001.
[30] P. Dorenbos, J. T. M. De Haas, and C. W. E. Van Eijk, "Non-proportionality in the scintillation response and the energy resolution obtainable with scintillation crystals," *IEEE Transactions on Nuclear Science***,** vol. 42**,** pp. 2190-2202, 1995.

[31] K. W. Kramer, P. Dorenbos, H. U. Gudel, C. W. E. van Eijk "Development and characterization of highly efficient new cerium doped rare earth halide scintillator materials," *J. Mater. Chem*., vol. 16, pp. 2776, 2003.
[32] E. V. D. van Loef, P. Dorenbos, C. W. E. van Eijk, K. Kramer, H. U. Gudel, "High-energy-resolution scintillator: Ce^{3+} activated $LaBr_3$", *Appl. Phys. Lett*., vol. 79, pp. 1573-1575, 2001.
[33] N. J. Cherepy, G. Hull, A. Drobshoff, S.A. Payne, E. van Loef, C. Wilson, K. Shah, U.N. Roy, A. Burger, L.A. Boatner, W-S Choong, W.W. Moses "Strontium and Barium Iodide High Light Yield Scintillators," *Appl. Phys. Lett.* **92**, 083508, 2008.

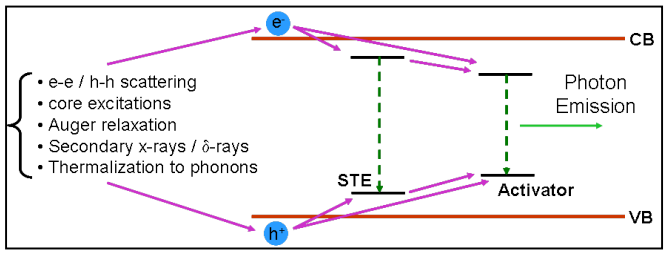

Fig. 1: Basic physical processes involved in scintillation.

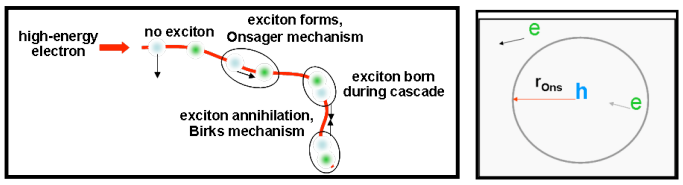

Fig. 2: Notional depictions of carrier and exciton interactions during track formation (left), and the Onsager mechanism (right). Electrons and holes are differentiated by color.

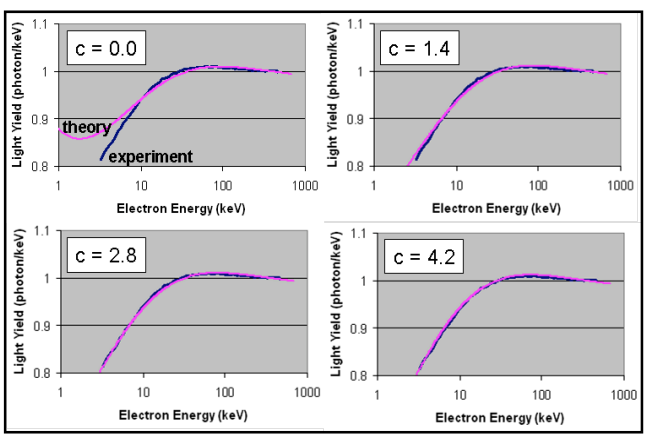

Fig. 3: Comparison of best-fits to $LaBr_3(Ce)$ for several c values.

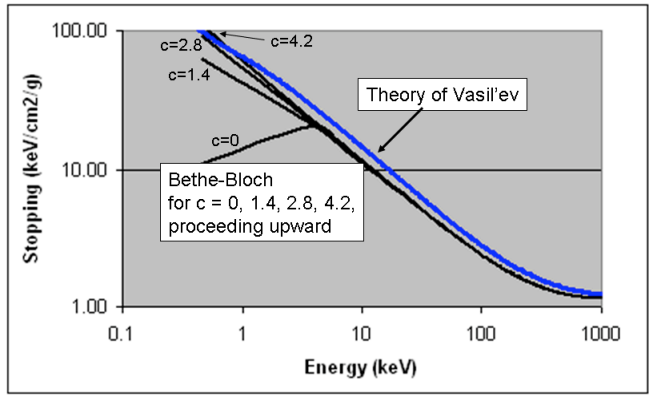

Fig. 4: Comparison of Bethe-Bloch equation (adjusted using c = 0, 1.4, 2.8 and 4.2), with the theory of stopping in NaI(Tl) by Vasil'ev [19].

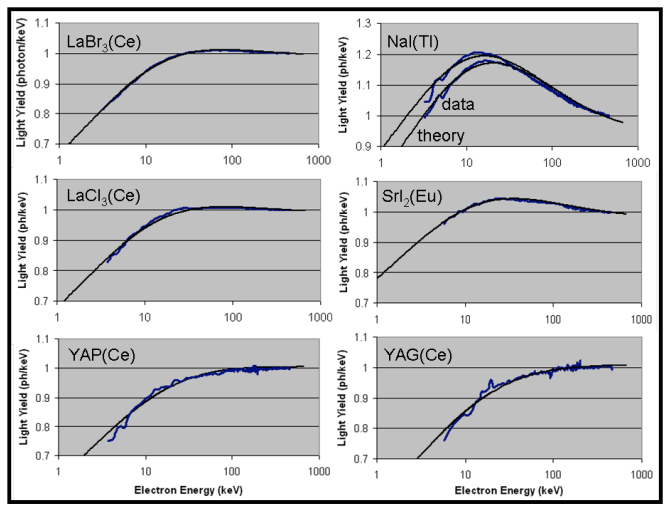

Fig. 5: Fits to nonproportionality data, for the parameters reported in Table I, where two different samples of NaI(Tl) were tested [25]. The light yields are normalized to unity for highest energies tested.

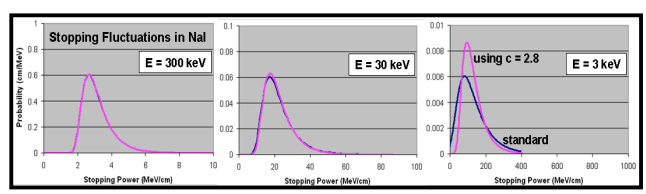

Fig. 6: Calculations of Landau distributions for three electron energies in NaI, with and without inclusion of the cI term (using c=0 and c=2.8).